ISSN 1070-3284, Russian Journal of Coordination Chemistry, 2014, Vol. 40, No. 9, pp. 617–626. © Pleiades Publishing, Ltd., 2014.

Syntheses and Structural Determination of Mononuclear Nine-Coordinate $(MnH)[Gd^{III}(EDTA)(H_2O)_3] \cdot 4H_2O$ and 2D Ladder-Like Binuclear Nine-Coordinate $(MnH)_2[Gd_2^{III}(H_2TTHA)_2] \cdot 4H_2O$[1]

C. C. Ma, Y. Li, J. Wang*, D. Y. Kong, C. Qin, and Q. Wu

Department of Chemistry, Liaoning University, Shenyang, 110036 P.R. China

**e-mail: wangjuncomplex890@126.com*

Received January 20, 2014

Abstract—Two title rare earth metal coordination compounds, $(MnH)[Gd^{III}(Edta)(H_2O)_3] \cdot 4H_2O$ (**I**) and $(MnH)_2[Gd_2^{III}(H_2Ttha)_2] \cdot 4H_2O$ (**II**), where Mn = methylamine, H_4Edta = ethylenediamine-N,N,N',N'-tetraacetic acid, H_6Ttha = triethylenetetramine-N,N,N',N'',N''',N'''-hexaacetic acid), have been successfully synthesized through direct heating reflux and characterized by FT-IR spectroscopy, thermal analysis and single-crystal X-ray diffraction techniques. In complex **I**, the Gd^{3+} ion is nine-coordinated by an Edta ligand and three water molecules, yielding a pseudo-monocapped square antiprismatic (MC-SAP) conformation. Complex **I** crystallizes in the orthorhombic crystal system with space group *Fdd2*. The cell dimensions are as follows: a = 19.5207(17), b = 35.387(3), c = 12.5118(11) Å, and V = 8642.8(13) Å^3. The central Gd^{3+} ion of **II** is also nine-coordinate, forming tricapped trigonal prismatic (TC-TP) conformation with three amine nitrogen atoms and six oxygen atoms. Complex **II** crystallizes in the monoclinic crystal system with $P2/c$ space group. The crystal data are as follows: a = 14.4301(13), b = 11.2400(11), c = 17.7102(16) Å, β = 112.606(2)°, and V = 2651.8(4) Å^3. There retain outer-protonated and inner-protonated carboxyl oxygen atoms in the $[Gd_2^{III}(H_2Ttha)_2]^{2-}$ complex anion. In **II**, there are only one type of methylamine cation (MnH^+) as the counter ion, which connects $[Gd_2^{III}(H_2Ttha)_2]^{2-}$ complex anions and lattice water molecules through hydrogen bonds, leading to the formation of 2D ladder-like layer structure.

DOI: 10.1134/S1070328414080065

INTRODUCTION

Owing to the particular physical and chemical properties, rare earth metals are usually selected to synthesize the metal-organic frameworks used in gas storage, adsorption, catalysis and separation [1–8]. In addition, some radioactive rare earth metal ions, for instance, $^{165}Dy^{3+}$ and $^{166}Ho^{3+}$ ions, due to the desirable radioactive characteristics, their corresponding complexes become excellent candidates for radiation synovectomy and radioimmunotherapy [9–11]. The Er(III) complexes play an important role in the production and development of laser fields [12]. Tb^{3+} ion, with a variety of organic ligands, is very popular as luminescent probes for the development of fluoroimmuno-assays [13, 14]. High energy β-emitter of Y^{3+} ion, represents significant superiority in the treatment of larger tumor [15, 16]. What's more, because there are seven high-spin single electrons in the *f*-orbits of Gd^{3+} ion, the most in all the rare earth metal ions [17–24], many Gd(III) complexes are used as contrast agents for magnetic resonance imaging (MRI) diagnoses. Recently, much betterment has been made for developing to cellular and molecular level [25], such as Gd^{3+} ion contract agents, nanoparticles based on colloidal lipid systems have been employed successfully to do cell labeling, using Gd-DTPA and $MnCl_2$ multiple MRI contrast agents to reveal detailed cytoarchitecture [26, 27]. In general, when most Gd(III)-based contract agents were synthesized the aminopolycarboxly acids would be taken as ligands, which can form extraordinarily stable and water-soluble complexes with metal ions [28–30]. It maks the Gd(III) complexes with aminopolycarboxylic acid ligands have more widely application in the field of medicine. Due to the major role of Gd(III) complexes played in biology activities, hence, we think it makes sense to study the molecular structure and coordinate structure of more Gd(III) complexes with aminopolycarboxylic acid ligands.

A series of Gd(III) complexes with Edta and Ttha ligands have been reported by our laboratory, such as $K[Gd^{III}(Edta)(H_2O)_3] \cdot 5H_2O$ (H_4Edta = ethylene-

[1] The article is published in the original.

diamine-N,N,N',N'-tetraacetic acid) [31], $Na_6[Gd^{III}_2(Ttha)_2] \cdot 8H_2O$ (H_6Ttha = triethylenetetramine-N,N,N',N'',N''',N'''-hexaacetic acid) [32] and $(EnH_2)_3[Gd^{III}(Ttha)]_2 \cdot 11H_2O$ [32]. By comparative analysis, it was found that, either Gd–Edta or Gd–Ttha complex, the coordination number all is nine. However, the coordinate structure and molecular structure are entirely different. The $K[Gd^{III}(Edta)(H_2O)_3] \cdot 5H_2O$ has a mononuclear molecular structure with pseudo-monocapped square antiprismatic (MC-SAP) conformation [31]. And the $(EnH_2)_3[Gd^{III}(Ttha)]_2 \cdot 11H_2O$ has two independent mononuclear structural units, and the GdN_4O_5 part in each $[Gd^{III}(Ttha)]^{3-}$ complex anion adopts a MC-SAP polyhedron [32]. However, the $Na_6[Gd^{III}_2(Ttha)_2] \cdot 8H_2O$ has a binuclear molecular structure, and the GdN_3O_6 part in each $[Gd^{III}_2(Ttha)_2]^{6-}$ complex anion adopts a pseudo-tricapped trigonal prismatic (TC-TP) geometry [32]. Therefore, our studies showed that the molecular structures and coordinate structures of rare earth metal complexes with aminopolycarboxylic acid ligands sometimes not only related to the shape of ligands but also the counter ion species. In order to make in-depth our research, we want to know how the organic amine ion and ligand species generate the effects upon coordination number, coordinate structure, space group, molecular structure and crystal structure. As well as known, the organic amine can be regarded as the part of the amino acid, the research of interactions between organic amine with rare earth metal complex anions is significant for the exploration of their bioactivities and targets.

It is well known, aminopolycarboxylic acid can form extraordinarily stable and water-soluble complexes with rare earth metal ions [33, 34]. So, in this article, two aminopolycarboxylic acids, H_4Edta and H_6Ttha, were chosen as ligands and methylamine as counter ion, two novel rare earth metal complexes with aminopolycarboxylic acid ligands, namely, $(MnH)[Gd^{III}(Edta)(H_2O)_3] \cdot 4H_2O$ (**I**) and $(MnH)_2[Gd^{III}_2(H_2Ttha)_2] \cdot 4H_2O$ (**II**), were successfully synthesized. As expected, they both adopt nine-coordinate structure. However, due to the different ligands, **I** and **II** have different molecular structures and coordinate structures. Complex **I** adopts a mononuclear nine-coordinate MC-SAP geometry and the binding between MnH^+ with $[Gd^{III}(Edta)(H_2O)_3]^-$ is reviewed, providing the basis for the interaction of Gd(III) complexes with various biomolecules. While the polymeric **II**, being different from complexe **I**, adopts a binuclear nine-coordinate TC-TP geometry. In addition, four protons do not dissociate from the carboxyl oxygen atoms of Ttha ligand and formed two outer-protonated and two inner-protonated carboxyl oxygen atoms in the $[Gd^{III}_2(H_2Ttha)_2]^{2-}$ complex anion. What's more, complex **II** adopts a 2D ladder-like network through hydrogen bonds formed between methylamine and $[Gd^{III}_2(H_2Ttha)_2]^{2-}$ complex anions. Therefore, it can be conclused that the ligand structures and counter ions play a crucial role on the coordinate structure of rare earth metal complexes.

EXPERIMENTAL

Synthesis of I. H_4Edta (A.R., Beijing SHLHT Science & Trade Co., Ltd., China) (1.4607 g, 5.0 mmol) was added to 100 mL warm water and Gd_2O_3 powder (99.999%, Yuelong Rare Earth Co., Ltd., China) (0.9062 g, 2.5 mmol) was added slowly to the above warm H_4Edta solution. After the mixture had been stirred and refluxed for 15.0 h, the solution became transparent, and then the pH value was adjusted to 6.0 by dilute methylamine (Mn) solution. Finally, the solution was concentrated to 25 mL and placed in dark desiccator. A light yellow crystal appeared after three weeks at room temperature. The yield was 76%.

$C_{11}H_{32}N_3O_{15}Gd$ (**I**)

anal. calcd., %:	Gd, 34.79;	C, 21.88;	H, 5.34;	N, 6.96.
Found, %:	Gd, 34.85;	C, 21.89;	H, 5.32;	N, 6.98.

Synthesis of II. H_6Ttha (A.R., Beijing SHLHT Science & Trade Co., Ltd., China) (2.4723 g, 5.0 mmol) was added to 100 mL warm water and Gd_2O_3 powder (99.99%, Yuelong Rare Earth Co., Ltd., China) (0.9062 g, 2.5 mmol) was added to above warm H_6Ttha solution slowly. The solution became transparent after the mixture had been stirred and refluxed for 13.0 h. And then the pH value was also adjusted to 6.0 by dilute methylamine (Mn). Finally, the solution was concentrated to 25 mL and placed in dark desiccator. A yellow crystal appeared after three weeks at room temperature. The yield was 79%.

$C_{38}H_{72}N_{10}O_{28}Gd_2$ (**II**)

anal. calcd., %:	Gd, 22.75;	C, 31.88;	H, 5.06;	N, 9.78.
Found, %:	Gd, 21.97;	C, 31.88;	H, 5.07;	N, 9.78.

Elemental analyses (C, H, and N) were determined by THERMO flash EA 1112 type analyzer instrument, and the Gd(III) was analysized by means of oxalate titration and thermal analysis. FT-IR spectra were determined by a Schimadza-IR 408 spectrophotometer (samples were skived and pressed to the slices with KBr). TG curves of **I** and **II** samples were determined by Mettler–Toledo 851 thermogravimetric analyzer in the presence of air (20 mL min^{-1}) from room temperature to 800°C at a heating rate of 20°C min^{-1}.

X-ray structure determination. X-ray intensity data of **I** and **II** samples were collected on a Bruker SMART CCD type X-ray diffractometer system with graphite-monochromatized MoK_α radiation (λ = 0.71073 Å) at 298(2) K using φ–ω scan tech-

Table 1. Crystal data and structure refinement for **I** and **II**

Parameter	Value	
	I	**II**
Formula weight	603.65	1431.56
Temperature, K	298(2)	298(2)
Wavelength, Å	0.71073	0.71073
Crystal system	Orthorhombic	Monoclinic
Space group	*Fdd*2	*P*2/*c*
Unit cell dimensions:		
a, Å	19.5207(17)	14.4301(13)
b, Å	35.387(3)	11.2400(11)
c, Å	12.5118(11)	17.7102(16)
β, deg	90	112.606(2)
Volume, Å^3	8642.8(13)	2651.8(4)
Z	16	2
ρ_{calcd}, mg/m^3	1.856	1.793
Absorption coefficient, mm^{-1}	3.146	2.578
F(000)	4848	1444
Crystal size, mm	0.45 × 0.40 × 0.27	0.12 × 0.06 × 0.04
θ Range for data collection, deg	2.38 to 25.02	2.94 to 25.02
Limiting indices	$-19 \le h \le 22$, $-40 \le k \le 41$, $-12 \le l \le 14$	$-17 \le h \le 17$, $-13 \le k \le 11$, $-20 \le l \le 20$
Reflections collected	9375	12466
Independent reflections (R_{int})	3243 (0.1695)	4632 (0.2524)
Completeness to θ_{max}, %	98.3	98.8
Max and min transmission	0.4838 and 0.3318	0.9039 and 0.7472
Goodness-of-fit on F^2	1.146	1.019
Final *R* indices ($I > 2\sigma(I)$)	$R_1 = 0.0885$, $wR_2 = 0.2009$	$R_1 = 0.1033$, $wR_2 = 0.1830$
R indices (all data)	$R_1 = 0.1415$, $wR_2 = 0.2603$	$R_1 = 0.1819$, $wR_2 = 0.2016$
Largest difference peak and hole, *e* Å^{-3}	3.343 and −1.690	2.349 and −1.551
Absorption correction	Empirical	
Refinement method	Full-matrix least-squares on F^2	

nique in the range of $1.72° \le \theta \le 26.00°$. Their structures were solved by direct methods. All non-hydrogen atoms were refined anisotropically by full-matrix least-squares methods. All the calculations were performed by the SHELXTL-97 program on PDP11/44 and Pentium MMX/166 computers. The crystal data and structure refinement for two complexes were listed in Table 1. And the selected bond distances and bond angles of two complexes were listed in Table 2.

Supplementary material has been deposited with the Cambridge Crystallographic Data Centre (nos. 966211 (**I**) and 966210 (**II**); deposit@ccdc.cam.ac.uk or http://www.ccdc.cam.ac.uk).

Table 2. Selected bond distances (Å) and angles (deg) of **I** and **II**

Bond	*d*, Å	Bond	*d*, Å	Bond	*d*, Å
		I			
Gd(1)–O(1)	2.40(2)	Gd(1)–O(7)	2.41(2)	Gd(1)–O(11)	2.461(18)
Gd(1)–O(3)	2.41(2)	Gd(1)–O(9)	2.49(2)	Gd(1)–N(1)	2.69(2)
Gd(1)–O(5)	2.42(2)	Gd(1)–O(10)	2.530(15)	Gd(1)–N(2)	2.67(2)
		II			
Gd(1)–O(1)	2.397(13)	Gd(1)–O(7)	2.647(14)	Gd(1)–N(1)	2.593(16)
Gd(1)–O(3)	2.362(14)	Gd(1)–O(9)	2.446(11)	Gd(1)–N(2)	2.642(14)
Gd(1)–O(5)	2.366(12)	Gd(1)–O(11)	2.404(14)	Gd(1)–N(3)	2.721(15)
Angle	ω, deg	Angle	ω, deg	Angle	ω, deg
		I			
O(1)Gd(1)O(3)	129.7(7)	O(3)Gd(1)O(11)	72.3(6)	O(7)Gd(1)N(1)	113.0(8)
O(1)Gd(1)O(5)	77.2(7)	O(3)Gd(1)N(1)	63.3(7)	O(7)Gd(1)N(2)	65.1(8)
O(1)Gd(1)O(7)	137.0(7)	O(3)Gd(1)N(2)	89.2(7)	O(9)Gd(1)O(10)	70.6(7)
O(1)Gd(1)O(9)	79.4(7)	O(5)Gd(1)O(7)	70.3(7)	O(9)Gd(1)O(11)	75.1(6)
O(1)Gd(1)O(10)	73.2(6)	O(5)Gd(1)O(9)	138.2(7)	O(9)Gd(1)N(1)	71.5(7)
O(1)Gd(1)O(11)	142.3(7)	O(5)Gd(1)O(10)	69.6(7)	O(9)Gd(1)N(2)	138.2(8)
O(1)Gd(1)N(1)	66.8(8)	O(5)Gd(1)O(11)	104.4(8)	O(10)Gd(1)O(11)	72.3(6)
O(1)Gd(1)N(2)	77.0(8)	O(5)Gd(1)N(1)	127.3(8)	O(10)Gd(1)N(1)	128.6(6)
O(3)Gd(1)O(5)	140.7(7)	O(5)Gd(1)N(2)	67.7(8)	O(10)Gd(1)N(2)	132.1(7)
O(3)Gd(1)O(7)	71.3(7)	O(7)Gd(1)O(9)	143.2(7)	O(11)Gd(1)N(1)	127.7(7)
O(3)Gd(1)O(9)	80.1(7)	O(7)Gd(1)O(10)	118.2(7)	O(11)Gd(1)N(2)	139.3(7)
O(3)Gd(1)O(10)	138.6(6)	O(7)Gd(1)O(11)	74.6(7)	N(1)Gd(1)N(2)	67.7(8)
		II			
O(1)Gd(1)O(3)	131.1(5)	O(3)Gd(1)N(1)	65.8(5)	O(7)Gd(1)N(2)	120.8(4)
O(1)Gd(1)O(5)	72.1(5)	O(3)Gd(1)N(2)	73.1(5)	O(7)Gd(1)N(3)	61.3(4)
O(1)Gd(1)O(7)	142.8(4)	O(3)Gd(1)N(3)	77.7(5)	O(9)Gd(1)O(11)	74.7(4)
O(1)Gd(1)O(9)	82.5(5)	O(5)Gd(1)O(7)	120.2(5)	O(9)Gd(1)N(1)	74.9(5)
O(1)Gd(1)O(11)	80.6(5)	O(5)Gd(1)O(9)	145.5(4)	O(9)Gd(1)N(2)	142.8(5)
O(1)Gd(1)N(1)	65.6(5)	O(5)Gd(1)O(11)	78.4(5)	O(9)Gd(1)N(3)	130.1(5)
O(1)Gd(1)N(2)	96.3(5)	O(5)Gd(1)N(1)	113.1(5)	O(11)Gd(1)N(1)	136.8(5)
O(1)Gd(1)N(3)	143.4(5)	O(5)Gd(1)N(2)	64.9(5)	O(11)Gd(1)N(2)	142.1(4)
O(3)Gd(1)O(5)	134.5(4)	O(5)Gd(1)N(3)	71.3(5)	O(11)Gd(1)N(3)	91.8(5)
O(3)Gd(1)O(7)	68.1(5)	O(7)Gd(1)O(9)	69.1(4)	N(1)Gd(1)N(2)	71.0(5)
O(3)Gd(1)O(9)	79.9(4)	O(7)Gd(1)O(11)	69.3(4)	N(1)Gd(1)N(3)	131.3(5)
O(3)Gd(1)O(11)	135.8(5)	O(7)Gd(1)N(1)	125.0(5)	N(2)Gd(1)N(3)	68.2(5)

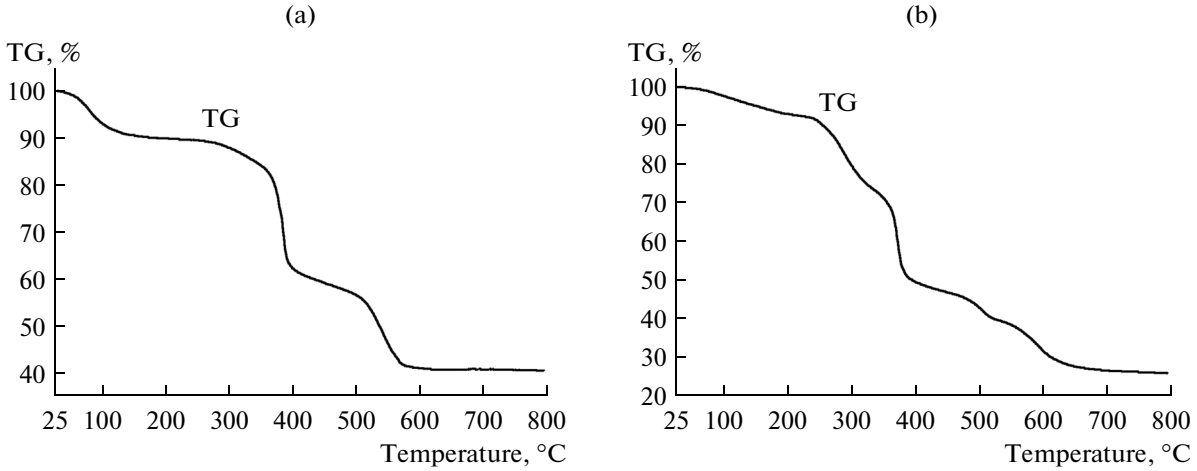

Fig. 1. TG curves of **I** (a) and **II** (b).

RESULTS AND DISCUSSION

A comparison of the FT-IR spectra between Edta ligand and **I** complex reveals considerable changes. The ν(C–N) at 1102 cm^{-1} is blue-shifted 48 cm^{-1} compared to H_4Edta (1054 cm^{-1}), which indicates that the amine nitrogen from Edta ligand coordinates to Gd^{3+} ion. The ν_{as}(COOH) in H_4Edta at 1686 cm^{-1} disappeared in complex **I**, showing that there are no free carboxylic groups in **I**. The ν_{as}(COO) at 1638 cm^{-1} of H_4Edta red-shifts to 1611 cm^{-1} and the ν_s(COO) at 1396 cm^{-1} of H_4Edta blue-shifts to 1402 cm^{-1} in complex **I**, confirming that all $-COO^-$ groups coordinate to Gd^{3+} ion too. There is a broad ν(OH) band of H_2O near 3432 cm^{-1} showing the existence of H_2O molecules in **I**.

A comparison of the IR spectra of Ttha ligand and **II** reveals considerable changes too. The ν(C–N) of **II** appears at 929 cm^{-1} shows a blue-shift (30 cm^{-1}) compared with that (899 cm^{-1}) of H_6Ttha ligand, indicating that the amine nitrogen atoms of the Ttha ligand are coordinated to the Gd^{3+} ion. The ν_{as}(COOH) band of H_6Ttha at 1736 cm^{-1} disappears in the FT-IR spectrum of complex **II**, the ν_{as}(COO) band of complex at 1606 cm^{-1} shows a blue-shift (136 cm^{-1}) compared with 1470 cm^{-1} of the H_6Ttha ligand, and ν_s(COO) of complex **II** at 1403 cm^{-1} reveals a red-shift (9 cm^{-1}) compared with 1414 cm^{-1} of the H_6Ttha ligand. These changes confirm that the oxygen atoms from carboxyl groups of the Ttha ligand are also coordinated to the Gd^{3+} ion. Also there is a broad ν(OH) band near 3433 cm^{-1}, presenting the existence of H_2O molecules in complex **II**.

The TG curve of **I** roughly shows a three-stage decomposition pattern (Fig. 1a). The first stage weight loss is about 8.42% from room temperature to 118°C, which corresponds to the expulsion of methylamine molecule. From 118 to 276°C, there is little weight loss, which means that the crystal structure is stable until 276°C. The second weight loss of 13.56% from 276 to 380°C should correspond to the expulsion of lattice water molecules. Then, the sample decomposes gradually and the decomposition is completed at 800°C, and the corresponding weight loss is about 37.93%. The total weight loss ratio of organic Ttha ligand should be about 59.91% according to the mass loss calculation. It is estimated that the remainder is mainly Gd_2O_3 as well as carbonate.

The thermal decomposition process of complex **II** is similar to that of complex **I** with three-stage decomposition pattern. The first thermal decomposition happens from 25 to 250°C (Fig. 1b). In this step the weight loss ratio is about 8.98%, which corresponds to the releasing of Mn molecules. The second weight loss (12.35%) from 250 to 310°C corresponds to the expulsion of lattice water molecules in complex **I**. Then, the sample decomposes gradually and the decomposition is completed at 800°C. The corresponding weight loss is about 52.44%. The total weight loss ratio of organic ttha ligand should be about 73.77% according to the mass calculation, which demonstrates that the corresponding final remainder is mainly Gd_2O_3 as well as carbonate.

Complex **I** has a mononuclear molecular structure (Fig. 2a). The centre metal Gd^{3+} ion is nine coordinated by two nitrogen atoms and seven oxygen atoms, four of these oxygen atoms are from the same Edta ligand and the other three are from three coordinated water molecules, yielding a slightly distorted MC-SAP polyhedron. It gives some similar findings previously reported, for instance, $Na[Gd^{III}(Edta)(H_2O)_3] \cdot 5H_2O$ [35], $NH_4[Ho^{III}(Edta)(H_2O)_3] \cdot 1.5H_2O$ [36] $K[Dy^{III}(Edta)(H_2O)_3] \cdot 3.5H_2O$ [37], and $K[Sm^{III}(Edta)(H_2O)_3] \cdot 2H_2O$ [38].

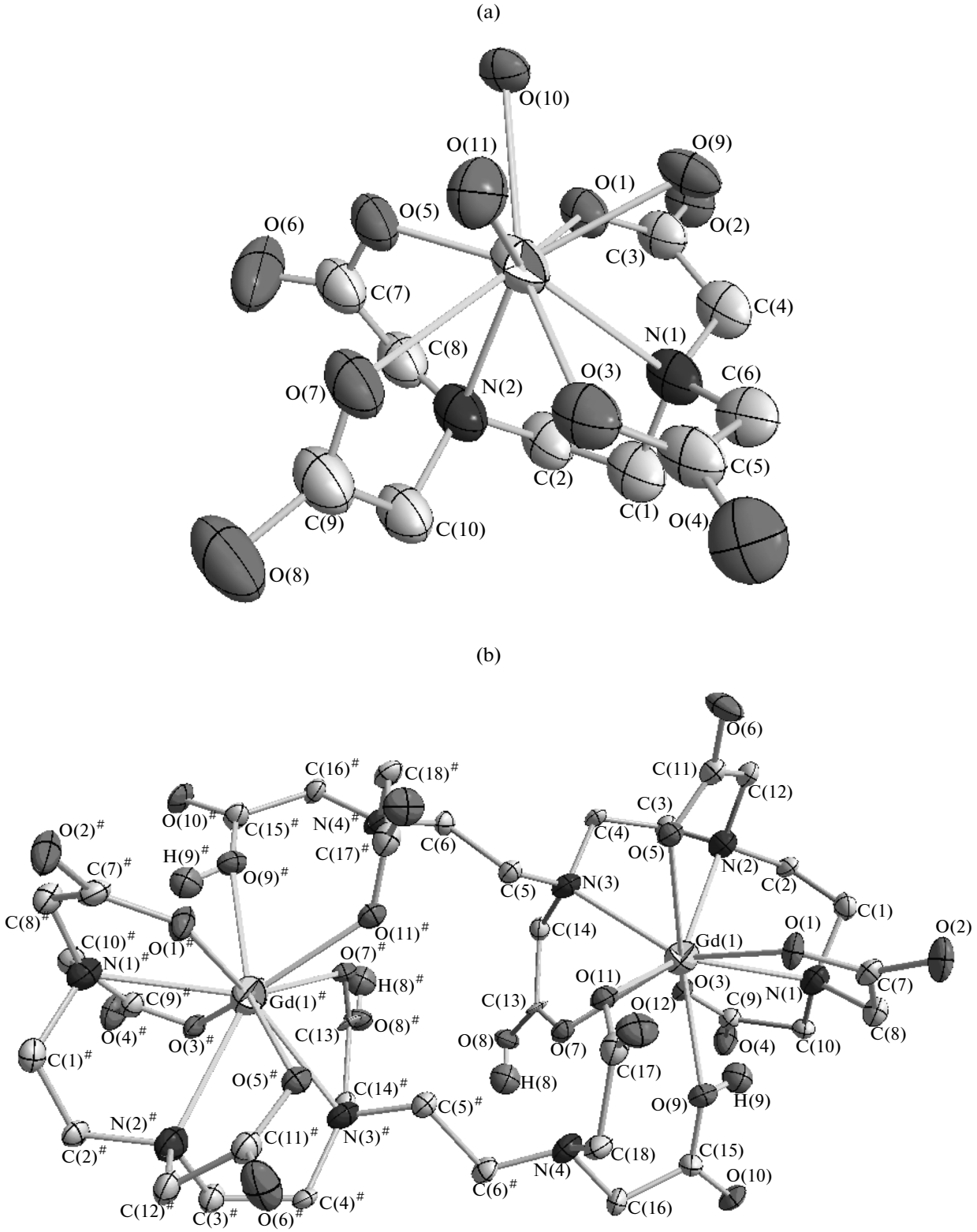

Fig. 2. Molecular structures of **I** (a) and **II** (b).

The coordination polyhedron of the $[Gd^{III}(Edta)(H_2O)_3]^-$ complex anion adopts nine-coordinate MCSAP geometry, a common conformation for nine-coordinate rare earth metal complexes with aminopolycarboxylic acid ligands (Fig. 3a). In the coordinate atoms around Gd^{3+} ion, the top tetragon plane is com-

posed of O(1), O(3), O(9), and N(2) atoms and the bottom tetragon plane is composed of O(5), O(7), O(10), and O(11), which form a square antiprism. The capped position above the top tetragon plane is occupied by N(1), which is different from some Edta-complexes, for instance, $NH_4[Eu^{III}(Edta)(H_2O)_3 \cdot H_2O$ [39], $K[Eu^{III}(Edta)(H_2O)_3] \cdot 3.5H_2O$ [40], and $Na[Y^{III}(Edta)(H_2O)_3] \cdot 5H_2O$ [41], whose capped position is generally occupied by a oxygen from a coordinated H_2O molecule. Because of the mutual repulsion between the top plane and the capped nitrogen atom, the bond length of Gd(1)–N(1) (2.69(2) Å) is the longest one of all the coordination bond lengthes. Moreover, the repulsion also results in the distance between two planes becoming shorter than that of normal square antiprismatic conformation. Hence, the conformation of the coordination polyhedron is not standard C_{4v} monocapped square antiprism, but a slightly pseudo one. The torsion angle between the two (top and bottom) quadrilateral planes is about 44.57°.

Furthermorebased on Fig. 3a, it can also be calculated that, to the top tetragon plane, the value of the trigonal dihedral angle between Δ(O(9)O(3)O(1)) and Δ(O(3)O(1)N(2)) is 5.63°, and between Δ(O(3)O(9)N(2)) and Δ(O(9)N(2)O(1)) is 6.22°. To the bottom tetragon plane, the trigonal dihedral angle between Δ(O(5)O(7)O(10)) and Δ(O(7)O(10)O(11)) is 13.52°, and between Δ(O(7)O(5)O(11)) and Δ(O(5)O(11)O(10)) is 12.28°. According to the viewpoint of Guggenberger and Muettertie [42], if the dihedral angle for nine-coordinate lanthanide complexes is between 0° to 26.4° the coordinate conformation can be regard as MC-SAP. For this reason, it can be firmly concluded that the GdN_2O_7 part indeed keeps a MC-SAP but distorted slightly.

In structure of **I**, the Gd(1)–O bond distances vary from 2.40(2) Å (Gd(1)–O(1)) to 2.530(15) Å (Gd(1)–O(10)), and the average value is 2.447(3) Å (Table 2). The Gd(1)–N bond lengths range between 2.67(2) Å (Gd(1)–N(2)) and 2.69(2) Å (Gd(1)–N(1)) with the average value of 2.68(2) Å. It is apparent that the Gd(1)–O bond distances are significantly shorter than the Gd(1)–N bond distances. From the above results we can come to the conclusion that the Gd(1)–O bonds are much stable than the Gd(1)–N bonds.

In one unit cell, there are sixteen molecules of **I** (Fig. 4). The complex molecules connect with lattice water and protonated methylamine cations (MnH^+) through hydrogen bonds. There are only one kind of MnH^+ (N(3)–C(11)) (Fig. 5). The N(3) connects with three O atoms, in which O(10) and O(11) are coordinated oxygen atoms from two crystal water molecules and O(8) are uncoordinated carboxyl O atoms from the other $[Gd^{III}(Edta)(H_2O)_3]^-$ complex anions. The hydrogen bond distances of N(3)···O(8), N(3)···O(10) and N(3)···O(11) are 2.705, 2.864, and 2.779 Å, respectively.

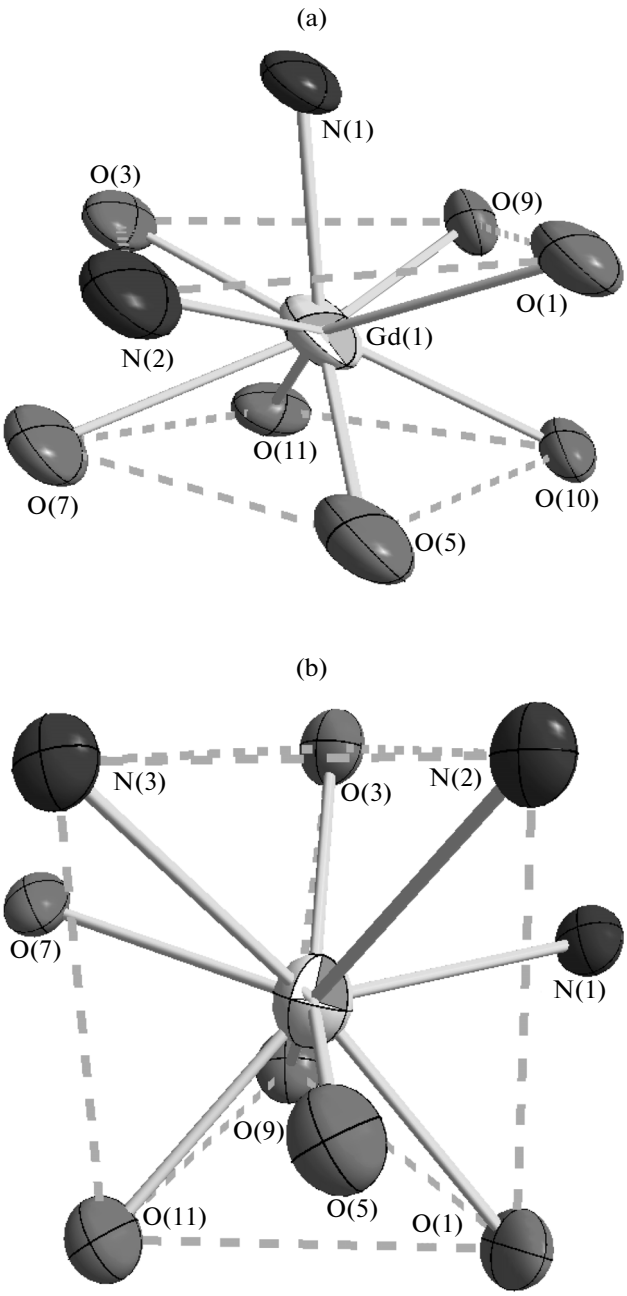

Fig. 3. Coordination polyhedron around Gd^{3+} ion in **I** (a) and **II** (b).

As seen from Fig. 2b, two Gd^{3+} ions and two Ttha ligands in **II** compose a nine-coordinate binuclear molecular structure. Gd(1) and Gd(1)$^{\#}$ are centrosymmetric (symmetry code: $^{1\#}$ $-x+1, -y+1, -z+1$). Each Gd^{3+} ion is coordinated with three amine nitrogen atoms and four oxygen atoms from one ttha ligand and two oxygen atoms from the other ttha ligand. It is similar to the findings that have been reported previously, such as $K_4[Tb_2^{III}(HTtha)_2] \cdot 14H_2O$ [43], $K_4[Y_2^{III}(HTtha)_2] \cdot 14H_2O$ [44], and $K_4[Sm_2^{III}(HTtha)_2] \cdot$

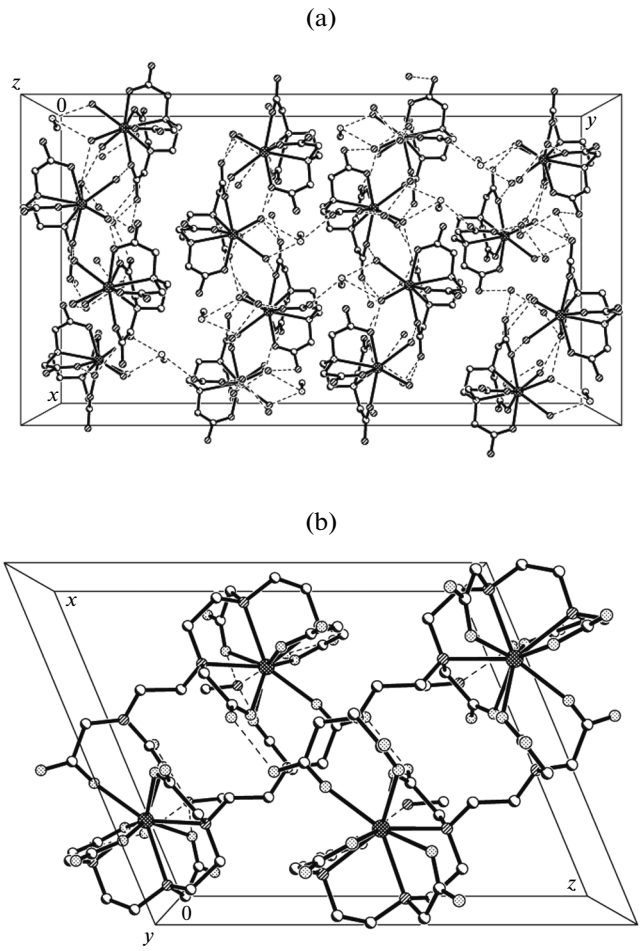

Fig. 4. Arrangement of **I** (a) and **II** (b) in unit cell (dashed lines represent intermolecular hydrogen bonds).

$14H_2O$ [45]. Moreover, it can be seen that four protons do not dissociate from the carboxyl oxygen atoms of ttha ligand and formed outer-protonated and inner-protonated carboxylic group in $[Gd_2^{III}(H_2Ttha)_2]^{2-}$ complex anions.

Figure 3b exhibits the coordination polyhedron of the $[Gd_2^{III}(H_2Ttha)_2]^{2-}$ complex anion. Obviously, the $Gd(1)N_3O_6$ part is binuclear nine-coordinate geometry with distorted TC-TP conformation. The coordinate atoms (O(3), N(2), and N(3); O(1), O(9), and O(11)) around Gd(1) form two approximately paralle trigonal planes. The dihedral angle between the two planes are 14.22°, forming a trigonal prism. The three capping positions above the side faces formed by O(1), O(11), N(2), and N(3); O(3), O(9), O(11), and N(3); O(1), O(3), O(9), and N(2) are occupied by O(5), O(7), and N(1), respectively. The total angles of O(5)Gd(1)O(7), O(5)Gd(1)N(1), and O(7)Gd(1)N(1) are 358.39° close to 360°, indicating that the Gd(1), O(5), O(7), and N(1) lie in the same plane.

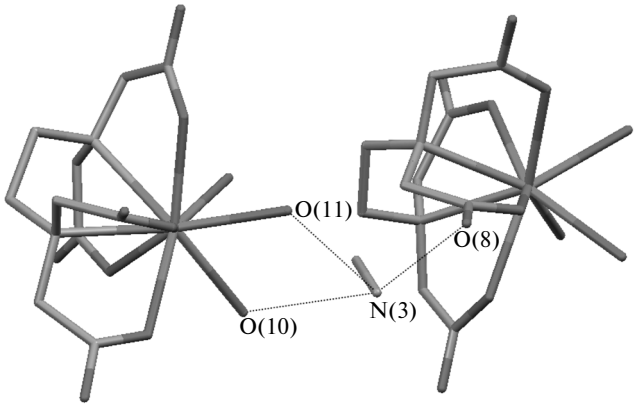

Fig. 5. Bindings between MnH^+ and $[Gd^{III}(Edta)(H_2O)_3]^-$ in **I** (dashed lines represent intermolecular hydrogen bonds).

Because of the repulsion between the capped atoms (O(5), O(7), and N(1)) and the planes (formed by O(1), O(11), N(2), and N(3); O(3), O(9), O(11), and N(3); O(1), O(3), O(9), and N(2)), the $Gd(1)N_3O_6$ part is not standard TC-TP conformation. To the O(1)O(11)N(2)N(3) square plane, the value of trigonal dihedral angle is 0.107° between Δ(N(3)O(1)O(11)) and Δ(N(2)N(3)O(1)); 0.105° between Δ(N(2)N(3)O(11)) and Δ(O(1)O(11)N(2)). To the O(3)O(9)O(11)N(3) square plane, the trigonal dihedral angle between Δ(N(3)O(3)O(11)) and Δ(O(3)O(11)O(9)) is 9.87°; between Δ(N(3)O(3)O(9)) and Δ(N(3)O(9)O(11)) is 10.34°. To the O(1)O(3)O(9)N(2) square plane, the trigonal dihedral angle between Δ(N(2)O(3)O(9)) and Δ(N(2)O(9)O(1)) is 12.69°; between Δ(O(3)N(2)O(1)) and Δ(O(3)O(1)O(9)) is about 11.19°. Of course, if the values of the trigonal dihedral angle trend to 0°, it is the greater chance of four atoms of dihedral angle in the same plane. Obviously, these data predict that four atoms of every side of triangular prism are almost located in the same plane, even though the $Gd(1)N_3O_6$ part is not standard TC-TP conformation. According to these calculated data, we can firmly draw a conclusion that the conformation of $Gd(1)N_3O_6$ in the $[Gd_2^{III}(H_2Ttha)_2]^{2-}$ complex anion indeed keeps a TC-TP conformation but distort to a small extent.

The lengths of the Gd(1)–O bond in the wide range vary from 2.366(12) Å (Gd(1)–O(5)) to 2.647(14) Å (Gd(1)–O(7)), with the average value of 2.437(13) Å (Table 2). Since the coordinated oxygen atom O(9) is protonated, reducing coordination ability, the bond length of Gd(1)–O(9) 2.446(11) Å is longer than the average value of 2.437(13) Å. Then uncoordinated oxygen atom O(7) is protonated also, the O(8)–C(13) bond lengh (1.32(2) Å) is the longest and the bond length of Gd(1)–O(7) (2.647(14) Å) is the longest one of all the coordination bond lengthes. The Gd(1)–N bond distances vary from 2.593(16) Å (Gd(1)–N(1)) to 2.721(15) Å (Gd(1)–N(3)), with the average value

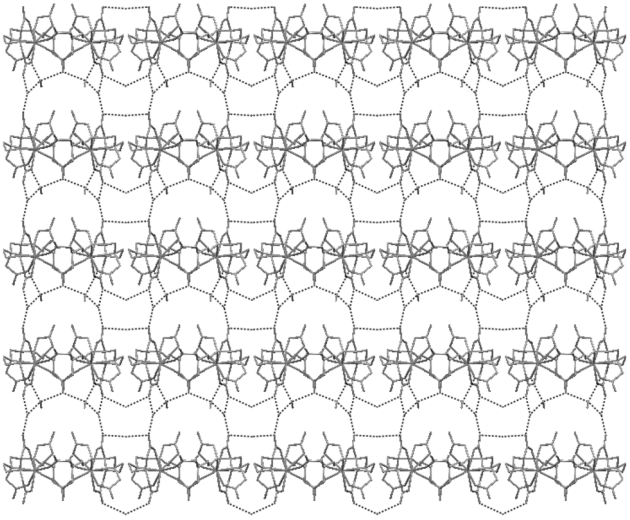

Fig. 6. Polyhedral view of the 2D ladder-like layered network of **II**.

of 2.652(15) Å, which are remarkably longer than the Gd(1)–O bond distances. It suggests that the O atoms coordinate to the central Gd^{3+} ion much stronger than the N atoms since the Gd(1)–O bond lengths are significantly shorter than the Gd(1)–N bond lengths. Because of protonation, the O(8) atom loses coordination ability, and the O(7) atom belonging to the protonated carboxylic group coordinates to Gd^{3+} ion making the O(7)C(13)C(14) bond angle change to 119.0(2)° close to 120°, causing the Gd–O(7)–C(13)–C(14)–N(3) pentagon to become rigid, further distorting the geometric configuration of **II**.

There are two molecules of **II** in a unit cell (Fig. 4b). The complex molecules connect with one another through hydrogen bonds and electrostatic forces with crystallization water and protonated methylamine cations (MnH^+). Furthermore, the hydrogen bonds play an important role in the construction of 2D planar structure of **II**. The $[Gd_2^{III}(H_2Ttha)_2]^{2-}$ complex anions are interconnected together by sharing the MnH^+ and lattice water molecule, forming infinite 1D chain along *x* aixs (Fig. 6). The hydrogen bond distances of O(15)···O(4), O(2)···O(14), O(2)···O(13), O(13)···N(5), and N(5)···O(12) are 2.905, 2.919, 2.783, 2.729, and 2.856 Å, respectively. Along *y* aixs, two neighboring $[Gd_2^{III}(H_2Ttha)_2]^{2-}$ complex anions are connected by sharing the MnH^+ and lattice water molecule, with N(5)···O(12), N(5)···O(13), N(5)···O(5), O(13)···O(4), and O(2)···O(13) hydrogen bond distances of 2.856, 2.729, 2.815, 2.689, and 2.783 Å, respectively, resulting in the formation of infinite 1D chain. The two 1D chains are linked by sharing the MnH^+ and lattice water molecule along *xy* plane, leading to the formation of loose 2D ladder-like network structure.

ACKNOWLEDGMENTS

The authors greatly acknowledge the National Science Foundation of China (21371084), Innovation Team Project of Education Department of Liaoning Province (LT2012001), Public Research Fund Project of Science and Technology Department of Liaoning Province (2012004001), Shenyang Science and Technology Plan Project (F12-277-1-15 and F13-316-1-51) and Science Foundation of Liaoning Provincial Education Department (L2011007) for financial support. The authors also thank our colleagues and other students for their participating in this work.

REFERENCES

1. Ma, S., Sun, D., Wang, X.S., et al., *Angew. Chem. Int. Ed.,* 2007, vol. 46, p. 2458.
2. Cairns, A.J., Perm, J.A., Wojtas, L., et al., *J. Am. Chem. Soc.,* 2008, vol. 130, p. 1560.
3. Zhang, J.P. and Chen, X.M., *J. Am. Chem. Soc.,* 2008, vol. 130, p. 6010.
4. Lee, J.Y., Olson, D.H., Pan, L., et al., *Adv. Funct. Mater.,* 2007, vol. 17, p. 1255.
5. Alvaro, M., Carbonell, E., Ferrer, B., et al., *Chem. Eur. J.,* 2007, vol. 13, p. 5106.
6. Xue, M., Zhu, G.S., Li, Y.X., et al., *Cryst. Growth Des.,* 2008, vol. 8, p. 2478.
7. Yu, X.H., Seo, S.Y., and Marks, T.J., *J. Am. Chem. Soc.,* 2007, vol. 129, p. 7244.
8. Amin, S.B. and Marks, T.J., *J. Am. Chem. Soc.,* 2007, vol. 129, p. 10102.
9. Verbruggen, A.M., *J. Nucl. Med.,* 1990, vol. 17, p. 346.
10. Sledge, C.B., Zuckerman, J.D., and Shortkroff, S., *J. Bone Joint Surg. Am.,* 1987, vol. 69, p. 970.
11. Volkert, W.A., Goeckeler, W.F., Ehrhardt, G.J., et al., *J. Nucl. Med.,* 1991, vol. 32, p. 174.
12. Ozolinsh, M. and Eichler, H.J., *Appl. Phys. Lett.,* 2000, vol. 77, p. 615.
13. Terai, T., Kikuchi, K., Iwasawa, S., et al., *J. Am. Chem. Soc.,* 2006, vol. 128, p. 6928.
14. Teotonio, E.E.S., Brito, H.F., Felinto, M.C.F.C., et al., *J. Mol. Struct.,* 2005, vol. 751, p. 85.
15. Deshpande, S.V., Denardo, S.J., Kukis, D.L., et al., *J. Nucl. Med.,* 1990, vol. 31, p. 473.
16. Miao, Y.B., Hoffman, T.J., and Quinn, T.P., *Nucl. Med. Biol.,* 2005, vol. 32, p. 485.
17. Efthimiadou, E.K., Katsarou, M.E., Fardis, M., et al., *Bioorg. Med. Chem. Lett.,* 2008, vol. 18, p. 6058.
18. Kupriyanov, V., Yang, Y., Gervai, P., et al., *J. Mol. Cell. Cardiol.,* 2008, vol. 44, p. 715.
19. Accardo, A., Tesauro, D., Aloj, L., et al., *Coord. Chem. Rev.,* 2009, vol. 253, p. 2193.
20. Vaccaro, M., Accardo, A., Errico, G.D., et al., *Biophys. J.,* 2007, vol. 93, p. 1736.
21. Chong, H.S., Song, H.A., Lim, S., et al., *Bioorg. Med. Chem. Lett.,* 2008, vol. 18, p. 2505.
22. Hak, S., Sanders, H.M.H.F., Agrawal, P., et al., *Eur. J. Pharm. Biopharm.,* 2009, vol. 72, p. 397.

23. Li, Z.F., Li, W.S., Li, X.J., et al., *Magn. Reson. Imaging,* 2007, vol. 25, p. 41.
24. Kubíček, V. and Tóth, É., *Adv. Inorg. Chem.,* 2009, vol. 61, p. 63.
25. Weissleder, R. and Mahmood, U., *Radiology.,* 2001, vol. 219, p. 316.
26. Hak, S., Sanders, H.M.H.F., Agrawal, P., et al., *Eur. J. Pharm. Biopharm.,* 2009, vol. 72, p. 397.
27. Huang, S.N., Liu, C., Dai, G.P., et al., *NeuroImage,* 2009, vol. 46, p. 589.
28. Egli, T., *J. Biosci. Bioeng.,* 2001, vol. 92, p. 89.
29. Sillanpää, M., Orama, M., Rämö, J., et al., *Sci. Total Environ.,* 2001, vol. 267, p. 23.
30. Rajesh, N.P., Meera, K., Perumal, C.K., et al., *Mater. Chem. Phys.,* 2001, vol. 71, p. 299.
31. Wang, J., Zhang, X.D., Fan, D.M., et al., *Chin. Rare Metals*, 2001, vol. 20, p. 224.
32. Wang, J., Hu, P., Liu, B., et al., *Russ. J. Coord. Chem.,* 2010, vol. 36, p. 232.
33. Egli, T., *J. Biosci. Bioeng.,* 2001, vol. 92, p. 899.
34. Sillanpaa, M., Orama, M., Ramo, J., et al., *Sci. Total Environ.,* 2001, vol. 267, p. 23.
35. Wang, J., Liu, Z.R., and Zhang, X.D., *Chin. J. Rare Earths.,* 2003, vol. 21, p. 16.
36. Wang, X.F., Liu, X.Zh., Wang, J., et al., *Russ. J. Coord. Chem.,* 2008, vol. 34, p. 134.
37. Liu, B., Gao, J., Wang, J., et al., *Russ. J. Coord. Chem.,* 2009, vol. 35, p. 422.
38. Liu, B., Hu, P., Wang, J., et al., *Russ. J. Coord. Chem.,* 2009, vol. 35, p. 758.
39. Wang, J., Zhang, X.D., Jia, W.G., et al., *Russ. J. Coord. Chem.,* 2004, vol. 30, p. 130.
40. Wang, J., Zhang, X.D., Zhang, Y., et al., *Russ. J. Coord. Chem.,* 2004, vol. 30, p. 850.
41. Wang, J., Wang, Y., Zhang, Zh.H., et al., *J. Struct. Chem.,* 2006, vol. 46, p. 895.
42. Guggenberger, L.J. and Muetterties, E.L., *J. Am. Chem. Soc.,* 1976, vol. 98, p. 7221.
43. Wang, J., Wang, Y., Zhang, Zh.H., et al., *J. Coord. Chem.,* 2006, vol. 59, p. 295.
44. Wang, J., Zhang, X.D., and Ma, R., *Chem. Res. Chin. Univ.,* 2002, vol. 18, p. 237.
45. Wang, J., Liu, X.Z., Zhang, Zh.H., et al., *J. Coord. Chem.,* 2006, vol. 59, p. 2103.